Fabrication and Characterization of Asymmetric Phosphoinositide-Containing Vesicles

A Major Qualifying Project Report Submitted to the Faculty of
WORCESTER POLYTECHNIC INSTITUTE
In partial fulfillment of the requirements for the
Degree of Bachelor of Science in Biochemistry

Written by:

_____

Nikayla Sims

Approved by:

_____

Dr. Gericke Arne

May 2021

Table of Contents

Acknowledgements

Abstract

The characterization of biological membranes has been improved through recent studies, which have brought about the development of biomimetic model membrane systems. Using these biomimetic systems, the lipid raft hypothesis has been established, which divides the membrane into liquid-ordered and liquid-disordered phases with lipids and proteins segregating into the phase with the appropriate physical properties. To further elucidate the interactions in the biological membrane, an asymmetric biological membrane system was developed to accurately mimic the asymmetry in native membranes. The link between phosphoinositide (PIP) mediated signaling and lipid rafts has been analyzed in multiple studies, and it has been suggested that PIPs cluster into lipid rafts. Investigations into the interactions between lipid rafts and PIP can provide potential mechanisms behind PIP signaling events in the biological membrane. The presence of cholesterol in lipid rafts is believed to stabilize the interactions between the head groups of the PIP and allow the acyl chains to pack tightly and therefore accumulate heavily in liquid-ordered domains. The segregation of PIP into specific phases can be influenced by interactions between the opposing leaflets in the membrane, this is known as interleaflet coupling. In order to further analyze the impacts of interleaflet coupling on PIP segregation into lipid raft domains, an asymmetric $PI(4,5)P_2$-containing model system was fabricated.

1. Introduction

The cell membrane is composed of proteins and amphipathic lipids that form associations driven by affinity, which allows the structure to be dynamic, and promotes rotational, translational, and transbilayer lipid movement [1]. The fluidity of the membrane is governed by the physical properties of the lipids and proteins in its composition. Phosphoinositides, a class of phospholipids, can be found in the cell membrane. A major class of Phosphoinositide is phosphatidylinositol-4,5-bisphosphate ($PI(4,5)P_2$), which accounts for about 1% of the phospholipids located in the plasma membrane [8]. $PI(4,5)P_2$ interacts with proteins and is responsible for mediating the pathways for cellular activity such as communication, cytoskeleton organization, and gene expression [2]. Previous research has indicated that lipid rafts organize signaling pathways regulated by phosphoinositides [7].

The concept of the existence of lipid rafts in the plasma membrane has been widely discussed. Lipid rafts can be classified as microdomains composed of cholesterol, sphingolipids, and proteins [9]. Multiple studies have hypothesized the nature of lipid rafts and their role within the plasma membrane. Rafts serve as scaffolds and aid in the regulation of cell signaling pathways and membrane trafficking, through the formation of liquid-ordered domains facilitated by cholesterol [10-11,22,24]. The lipid raft systems have been studied in symmetric vesicles, but biological membranes are vertically asymmetric. Therefore, studies have been conducted to simulate asymmetric vesicles to analyze these processes in biological conditions.

Lipid rafts have been hypothesized to induce the formation of phase-separated domains in the plasma membrane. The phases can be classified as liquid-ordered (l_o) and liquid-disordered (l_d), furthermore, it has been seen that signaling molecules and proteins tend to cluster in the liquid-ordered domains [20-21]. Additionally, the clustering of these molecules is affected by a phenomenon known as interleaflet coupling, which indicates that lipids in opposing leaflets can influence the molecular diffusion and domain formation in another leaflet [34]. Potentially, domain formation in either leaflet can encourage the accumulation of specific proteins or lipids that prefer specific phase environments.

Drawing conclusions from previous studies, this thesis hypothesizes that domains formed in the lipid rafts of the outer leaflet will promote the formation of a phosphoinositide-containing domains in the inner leaflet. The presence of cholesterol, which serves as a stabilizing agent will encourage the formation of these domains [25]. To investigate this hypothesis, an asymmetric giant unilamellar vesicle containing $PI(4,5)P_2$ was fabricated using the hemifusion method and analyzed using confocal microscopy.

2. Background

2.1 Fluid Mosaic Model/Properties of the Plasma Membrane

In 1972, two researchers, Singer and Nicholson formulated the fluid mosaic membrane hypothesis. They hypothesized that the cell membrane is composed of a variety of molecular components such as, lipids, proteins, and cholesterol that are always in motion. The main components of the membrane are phospholipids. This class of lipid is amphiphilic, indicating the presence of both hydrophilic (head) and hydrophobic (tail) components [16]. These properties allow for the membrane to arrange itself into a bilayer, where the hydrophobic tails form the inner layer, and the hydrophilic heads form the outer layer. The development of the fluid mosaic model allowed for the elucidation of collected data and the prediction of the outcomes in future experiments. Furthermore, about three decades after the development of this hypothesis there was evidence of lateral heterogeneity in the membrane [20].

In the years following this discovery, there have been additions to the fluid mosaic model to address the shortcomings of the original. An example of one improvement is the Mattress model, which tried to explain the heterogeneity of the plasma membrane. Specifically, this model helped to introduce the concept of lipid rafts [19].

2.1.2 Lipid Rafts

Drawing from the precedents set by the fluid mosaic model it was determined that the plasma membrane had liquid-ordered (l_o) and liquid disordered (l_d) phases. The liquid-ordered state is characterized by the tight packing of lipids while still maintaining lateral movement throughout the membrane. In contrast to the liquid-ordered phase, the liquid disordered phase is completely fluid and also allows for quick lateral movement throughout the membrane. The separation of the membrane into these phases encourages the formation of subdomains called lipid rafts [20,21]. The existence of these subdomains has been debated over the years, but there have been studies that worked to prove their existence [4,7,9,11].

The study of cholesterol-containing model membranes has aided in further advancing the understanding of the formation and segregation of these lipid rafts. Cholesterol is considered a major component of the membrane that promotes the formation of these domains [4]. Multiple studies have indicated that cholesterol regulates the formation of the liquid-ordered domain through its spatial organization. Sphingolipids/saturated acyl phospholipids and cholesterol form liquid-ordered domains based on favorable interactions encouraged by the biochemical and biophysical properties of cholesterol. Considered a membrane-active sterol it has been shown that cholesterol and similar sterols have structures that allow phospholipids/sphingolipids to pack tightly [22-24]. The hydrophobic and hydrophilic structural components of cholesterol allow for it to orient itself parallel to acyl chains in the membrane phospholipids. The proximity of cholesterol to these phospholipids potentially allows the interaction between the hydroxyl groups and promotes hydrogen bonding. This interaction may play a smaller role in the stabilization of

the phospholipid/cholesterol interaction as opposed to the van der Waals forces that are present between the acyl chain and sterol ring structure [25].

2.2 Lipid Model Membrane

Biological membranes are complex systems requiring simple models to better understand them. The complexity of the biological membrane makes it difficult to attribute specificity to processes that occur between proteins and their receptors, as there are non-specific lipid interactions that can interfere. The development of model systems has begun to allow the membrane to be broken into sub-domains that can then be studied under specific conditions [31]. These model systems can be tailored to specific sizes, geometries, and compositions [5]. Many model systems depict symmetric vesicle membranes and do not portray the distribution of lipids in the inner and outer leaflets of the membrane [18]. Despite the simplified demonstration of the plasma membrane, lipid model membranes give insight into the interactions of specific lipids within the system. Lipids are affected by peripheral and integral protein interactions, and these impacts are not depicted by the lipid model membranes. Therefore, it is important to be cognizant of the potential effects of the proteins in the plasma membrane.

Examples of lipid model membranes include multilamellar vesicles (MLV), small unilamellar vesicles (SUV), large unilamellar vesicles (LUV), giant unilamellar vesicles (GUV), supported lipid bilayers (SLB), and micelles. The previously mentioned model membranes can be used to determine the distribution of lipid rafts throughout the membrane. Solid supported lipid bilayers in particular have become a major model system used to further characterize the interactions within the membrane, due to their simple nature and planar geometry [32,36]. Three main methods to produce SLBs include vesicle fusion, Langmuir Blodgett/Schaefer, or lipid/detergent mixed micelle, and of these methods, vesicle fusion is the more simplistic option [33]. Vesicle fusion, as shown in Figure 1., relies on a variety of factors that impact the interaction between small or large unilamellar vesicles and a given substrate (glass, silica, etc.). The influence of these factors can impede the formation of the SLBs, specifically when the vesicle concentrations are more complex and closely resemble native membranes [33]. Furthermore, the interaction between the SLB and the substrate can decrease lipid mobility in the bottom leaflet of the membrane. Oftentimes, Fluorescence Recovery After Photobleaching (FRAP) is used to measure the fluidity of the SLB. Previous laboratories have determined that following FRAP only about 50% of the membrane is fluid and it is assumed that this is the top leaflet [36,37].
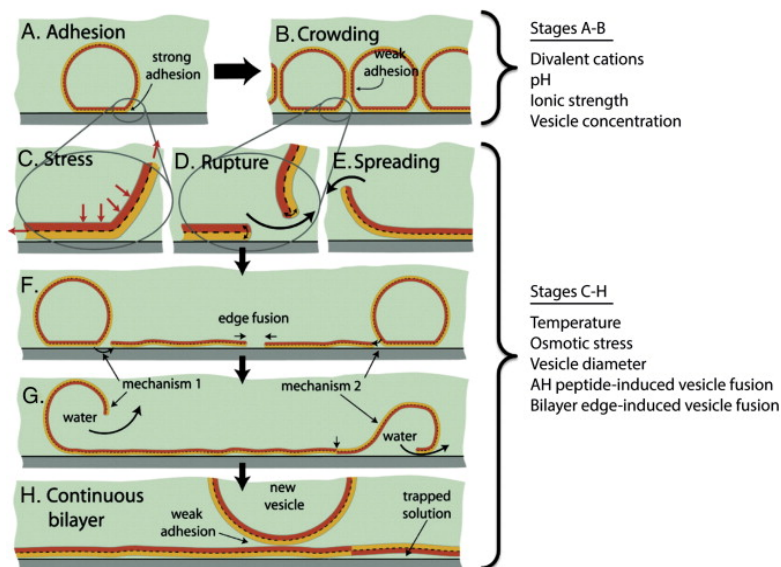
Figure 1. Vesicle fusion process. Figure borrowed from ref [32] depicting the formation of a supported lipid bilayer through the process of vesicle fusion. The stages of vesicle fusion can be impacted by several factors, as listed in the captions on the right.

2.3 Asymmetric GUVs

Interactions between the supported lipid bilayer and the giant unilamellar vesicles can be utilized to create asymmetric GUVs. As demonstrated in the Enoki & Feigenson paper [29], GUVs can undergo hemifusion through close interactions with SLBs formed through the vesicle fusion of small unilamellar vesicles. The development of asymmetric vesicle systems allows the examination of the interaction between the inner and outer leaflets due to interleaflet coupling. GUVs are a convenient model system, on account of their large size since they are large enough to be viewed under a confocal microscope, unlike SUV or LUV systems. GUV sizes can range from 10μm-100μm and provide information regarding the shape, fluidity, and domain formation when using confocal and fluorescent microscopy simultaneously [35].

2.4 Phosphoinositides/PI(4,5)P$_2$

Phosphoinositides are a class of phospholipids located in the cytoplasmic leaflet of the membrane. These acidic phospholipids make up <1% of the inner leaflet of the plasma membrane, while other phospholipids such as phosphatidylserine (PS) make up about 30% of the inner leaflet. Despite comprising only a small portion of the membrane, phosphoinositides play a major role within the cell. They are responsible for the regulation of many cell signaling pathways, such as cell proliferation, communication, gene expression, and cytoskeleton organization [2,36]. Defects in phosphoinositide metabolism can cause ailments such as cancer, cardiovascular disease, and autoimmune dysfunction [15].

Phosphoinositides are identified by the presence of an inositol ring, which can be phosphorylated to form seven variations of the phosphoinositide species [12]. Phosphoinositides have two hydrocarbon tails, arachidonate, and stearate, which are connected by a glycerol group to the inositol head group, which can be seen depicted in Figure 2. The phosphoinositide PI(4,5)P$_2$ is one of the major signaling lipids and plays an essential role within the plasma membrane. This PIP$_2$ molecule can be identified by its highly negative head group with an

electrostatic charge of ≤ -4 at biological pH [13]. Due to the electrostatic charge on PIP_2, they are more likely to form non-lamellar instead of lamellar lipid bilayers.
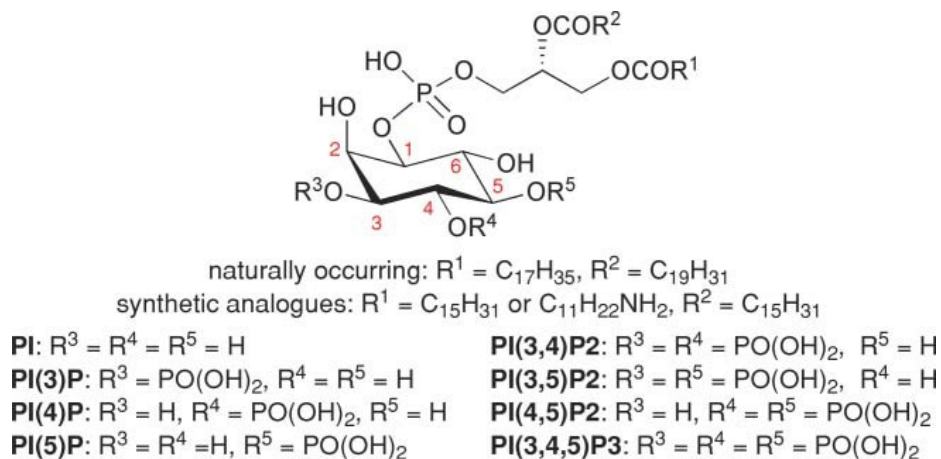

naturally occurring: $R^1 = C_{17}H_{35}$, $R^2 = C_{19}H_{31}$
synthetic analogues: $R^1 = C_{15}H_{31}$ or $C_{11}H_{22}NH_2$, $R^2 = C_{15}H_{31}$

PI: $R^3 = R^4 = R^5 = H$

PI(3)P: $R^3 = PO(OH)_2$, $R^4 = R^5 = H$

PI(4)P: $R^3 = H$, $R^4 = PO(OH)_2$, $R^5 = H$

PI(5)P: $R^3 = R^4 = H$, $R^5 = PO(OH)_2$

PI(3,4)P2: $R^3 = R^4 = PO(OH)_2$, $R^5 = H$

PI(3,5)P2: $R^3 = R^5 = PO(OH)_2$, $R^4 = H$

PI(4,5)P2: $R^3 = H$, $R^4 = R^5 = PO(OH)_2$

PI(3,4,5)P3: $R^3 = R^4 = R^5 = PO(OH)_2$

Figure 2. Phosphoinositide and the 7 phosphorylated derivatives Borrowed from ref [35].

2.4.1 Phosphoinositide and Lipid Raft Interaction

Lipid rafts serve as scaffolds for PIP_2 molecules allowing them to regulate a variety of signaling pathways [26]. These pathways are compartmentalized by concentrating PIP_2 within the raft domains and this provides spatial and temporal regulation [27]. Specifically, the presence of cholesterol in these microdomains aids in packing of these PIP_2 molecules. As previously mentioned, the hydrophobic and hydrophilic portions of cholesterol allow it to align itself parallel to the acyl chains of many membrane phospholipids serving as a barrier to electrostatic repulsion [25]. The effects of changes in cholesterol concentration on $PI(4,5)P_2$ behavior have been observed, and it has been shown that a decrease in cholesterol also decreases the lateral mobility of the plasma membrane and this occurs through the rearrangement of actin, which are regulated by PIP_2. Cholesterol depletion leads to the rearrangement of these PIPs and causes morphological changes in the plasma membrane, which in turn impact the fluidity of the membrane [7].

2.4.2 PI(4,5)P2 Organization

$PI(4,5)P_2$ has a 45° headgroup orientation that affects the orientation of the lipids surrounding the PIP_2. The rearranging effect of PIP_2 on surrounding lipids was observed in a DPPC membrane system. One study analyzed the tilting of the head group of DPPC to the membrane in the presence and absence of PIP_2. It was observed that when PIP_2 was within 7.5–9.5 Å, the DPPC exhibited a wider angle tilt distribution. This study hypothesized that the ability for PIP_2 to induce these rearrangements of surrounding lipids allows for it to generate an environment that promotes tighter packing and prevents vertical displacement by protein binding [14]. The negative charge of the head group allows PIP_2 to bind to proteins and peptides with

varying specificities [36]. Proteins containing the pleckstrin homology domain (PH Domain) have been shown to bind with a high affinity to PI(4,5)P$_2$ [38]. The specificity proteins have for PIP$_2$ allow it to engage in a variety of cellular functions and therefore it must be highly regulated. This order of regulation is accomplished by having these cellular events occur at localized pools of PIP$_2$ in the plasma membrane. The formation of these localized pools of PIP$_2$ can be induced by concentrations of multivalent cations such as, Ca^{2+} and Mg^{2+}. Previous studies have demonstrated that in the presence of Ca^{2+} the clustering of PIP$_2$ increases [39-40]. One study tested the effects of multivalent cation interactions on additional labeled lipids and found that Ca^{2+} mediated clustering is specific to PIP$_2$. These clustering effects have been seen in physiological conditions, implying that minimal amounts of Ca^{2+} can be used to induce clustering of PIP$_2$ in the plasma membrane [39].

2.6 Hypothesis

Utilizing the previously optimized protocol to fabricate GUVs through electroformation [28] the coupling behavior of the inner and outer membrane leaflets was investigated under specific conditions. This thesis continued the investigation of interleaflet coupling between phosphoinositide-cholesterol domains and lipid rafts. Asymmetric GUVs were fabricated using the hemifusion method, producing an inner leaflet that contained the Phosphoinositide and an outer leaflet containing the lipid raft mixture. Due to time constraints, the previous study was unable to test the registration of PI(4,5)P$_2$ when cholesterol was present in both the inner and outer leaflet mixtures. The stabilizing nature of cholesterol is assumed to encourage the registration of the PIP$_2$ with the liquid-ordered phase of the lipid raft mixture. The coupling of these two domains was quantified using fluorescence and confocal microscopy. A graphical representation of this hypothesis can be seen in Figure 3.
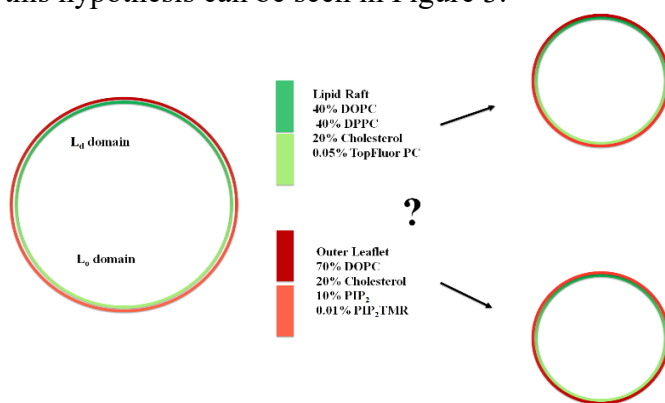

Figure 3. Graphical Representation of Hypothesis Asymmetric GUVs were fabricated with an inner leaflet containing a phase separated lipid raft mixture, and a phosphoinositide-containing outer leaflet. The inner leaflet is represented by the green region and the outer leaflet is represented by the red region. The dark green represents the liquid-disordered phase and light green represents the liquid-ordered phase. In this thesis it was hypothesized that the stabilizing nature of cholesterol would encourage the registration of PIP$_2$ into the liquid-ordered domain. This will be illustrated by a darker red region which signifies a higher concentration of PIP$_2$.

3. Methodology

Materials

DOPC (1,2-dioleoyl-sn-glycero-3-phosphocholine), DPPC (1,2- dipalmitoyl-sn-glycero -3- phosphocholine), PI(4,5)P$_2$ (phosphatidylinositol-4,5-bisphosphate), TopFluor PC (1-palmitoyl- 2-(dipyrrometheneboron difluoride)undecanoyl-sn-glycero-3- phospho-choline), TopFluor TMR PI(4,5)P$_2$ (1-oleoyl-2-(6-((4,4-difluoro-1,3-dimethyl-5- (4-me-thoxyphenyl)-4-bora-3a,4a-diaza-s- indacene-2-propionyl)amino) hexanoyl)-sn- gly-cero-3-phosphoinositol-4,5-bisphosphate) and cholesterol were purchased from Avanti Polar Lipids (Alabaster, AL). Indium tin oxide coated coverslips (22x22 mm, thickness #1.5, 70-100 ohms resistivity) were purchased from the SPI Supplies (Westchester, PA). Lab-Tek II4-well chambered coverglass was purchased from Thermo Fisher Scientific (Waltham, MA).

DOPC/DPPC/Cholesterol GUV Formation

Indium Tin Oxide (ITO) slides were rinsed with isopropanol and dried in an oven at 60°-70°C for 10 minutes. 10 µL of lipid mixture was spread evenly onto the ITO-coated surface of both coverslips using a 10 µL glass microsyringe. The slides were dried for 5 minutes under N$_2$ gas and then preheated in the oven for 30 minutes. The slides were placed ITO side inward on both sides of a 1.5 mm thick plastic spacer using vacuum grease. A Sucrose buffer (200mM sucrose, 1mM NaCl, 1mM Hepes, pH 7.4) was injected into the electroformation chamber. The slides were attached to an AC Power supply (Hewlett-Packard 3311A Function Generator) using conductive copper tape and alligator clips. Vesicles were electroformed at 70°C with an AC sine wave at 10 Hz and a 1.1 Vpp amplitude for 1 hour. After 1 hour, the Vpp was increased to 1.5 Vpp for 2 hours. To detach the vesicles, a 4Hz square waveform was applied for 1 hour. An oscilloscope was used to measure voltage and frequency throughout. Vesicles are left overnight to cool to room temperature and then stored in a centrifuge tube at 4°C for up to 3 days.

LUV Formation

LUVs were prepared via extrusion. The Lipid mixture (70% DOPC, 10% PIP$_2$, 20% Cholesterol, and 0.05% PIP$_2$ TMR) was dried under N$_2$ gas, then placed in a vacuum oven for $\geq$ 2 hours or overnight. Lipid mixture can stay in the oven for up to 48 hours. The lipid mixture was then rehydrated in 500 µL of buffer A (25 mM HEPES pH 7.4, 35 mM KCL, 50 mM NaCl for a total lipid concentration of 2.5 mM). Vesicles were extruded 33x through a 100 nm pore membrane and size was confirmed using a

Malvern Zetasizer. LUVs were diluted to 0.5 mM with 1 M NaCl and stored at 4°C for up to 1 week.

Supported Lipid Bilayer (SLB) Formation

Lab-Tek 4-well covered chamber glass slides were rinsed with a fresh preparation of 1 M KOH in ethanol, flushed with DI water, dried under N_2 gas, then subject to a plasma cleaner (Mercator Control Systems LF-5 Plasma System) with O_2 for 2 minutes. 500 μL of LUVs were added to the chamber wells and allowed to sit for 1 hour at room temperature. The SLB was washed by submerging the chamber wells in 2.5 L of MilliQ water and flushing each chamber with water using a syringe. The buffer in the chamber was replaced with buffer A while keeping the SLB hydrated. SLBs can be stored at 4°C for up to 5 days.

Asymmetric GUV Formation by Hemifusion

Asymmetric GUVs were prepared by hemifusion as described by Thais Enoki and Gerald Feigenson [6]. Buffer in the SLB chamber was replaced by buffer B (25 mM HEPES pH 7.4, 35 mM KCl, 50 mM NaCl, 1 mM $CaCl_2$) without dehydrating the SLB. 40-75 μL of GUVs were added to the SLB chamber in 5 μL aliquots and were allowed to settle for 5 minutes. GUVs were imaged briefly before moving forward to confirm they had settled on the SLB surface. 25-75X 5 μL aliquots of buffer C (25 mM HEPES pH 7.4, 25 mM KCl, 20 mM $CaCl_2$, 40 mM NaCl) were added to increase the Calcium concentration. In the chambers with GUVs, 50 μL of Buffer C was added to the chamber and mixed gently. The SLB chamber was allowed to sit for 30-45 minutes and the asymmetry of the GUVs was checked under the microscope. 1 mL of buffer D (25 mM HEPES pH 7.4, 25 mM EDTA, 40 mM NaCl) was added and the chamber to chelate calcium and stop hemifusion.

Determination of Calcium Concentration

The calcium-sensitive dye Rhod-5N was used to determine calcium concentration for the hemifusion experiments. A standard curve of calcium concentrations ranging from 0 (EDTA added) – 10 mM was created using $CaCl_2$ with 0.5 μM Rhod-5N in a pH 7.4 HEPES buffer. Samples from the hemifusion experiments were taken out and diluted to a final volume of 2 mL. Rhod-5N was added to a final concentration of 0.5 μM. The samples were measured in quartz cuvettes with a fluorimeter at 551 nm excitation. Emission was scanned over the range of 560- 700 nm.

Confocal Microscopy

Vesicles were imaged in the electroswelling chamber or the SLB well using a Zeiss LSM 510 confocal microscope with a 63x oil DIC objective. TopFluor TMR PI(4,5)P2 was excited with an

argon laser at 543 nm with 40% power and 40% transmission. TopFluor PC was excited with an argon laser at 40% power at 488 nm, 40% transmission. Microscope settings were kept consistent for comparison of fluorescence intensity in symmetric and asymmetric GUVs. Zeiss software and ImageJ were used to analyze the images captured.

Fluorescence Recovery after Photobleaching (FRAP)

FRAP was performed with the same confocal microscope as described above. Three image frames were collected with normal laser intensity, then the SLB was bleached with maximum laser intensity for 3 frames within a circular ROI with a radius of 7 μm. Following bleaching, 17 image frames were collected. Fluorescence intensity within the ROI was quantified using ImageJ software.

GUV Image Analysis

Fluorescence intensity analysis of GUVs was carried out in ImageJ as described by Thais Enoki and Gerald Feigenson [29]. Briefly, lines were drawn from the center of the GUV to the image frame. These lines were drawn at each degree around the circumference of the vesicle and fluorescence intensity was recorded for each point along the line. The maximum intensity, corresponding to the bilayer of the GUV was determined. For phase-separated GUVs, the fluorescence intensity of each phase was analyzed separately.

4. Results

4.1 GUV Formation in Low Salt Buffer

A moderate yield of GUVs was produced using the low salt buffer optimized by a previous MQP student [30]. This thesis did not compare the yield of GUVs in varying salt buffers. The GUVs produced in the low salt buffer were around 10-25μm in diameter. Despite having a moderate yield, the GUVs produced often formed clusters or multilamellar vesicles (MLVs).

4.2 Registration of PI(4,5)P$_2$

Demonstrated in Figure 6, following hemifusion the fluorescently labeled PIP$_2$ registered in the same region as TopFluor PC. Indicating that the PIP$_2$ registered in the liquid-disordered domain as opposed to the liquid-ordered domain as hypothesized. Figure 6. presents an example of a phase separated GUV and depicts two graphs that plot the fluorescence intensity of a two separate GUVs, the first image was captured before hemifusion occurred, and the second image was captured after hemifusion. The top graph shows a separation between the liquid-disordered (high intensity) and liquid-ordered (low intensity) of TopFluor PC. PIP$_2$TMR has not been introduced to the system as hemifusion has not occurred. The bottom graph shows a similar separation of TopFluor PC, which now also includes the intensity profile of PIP$_2$TMR following the initiation of hemifusion.

4.3 Asymmetry in Phase Separated and Non-Phase Separated GUVs

The asymmetry of the GUVs can be quantified by comparing the change in fluorescence intensity before and after hemifusion. An example of this can be seen in Figure 4. The bottom left graph in this figure plots the average max fluorescence intensity across a population of non-phase separated GUVs before (n=6) and after (n=6) hemifusion. The max fluorescence intensity of the TopFluor PC decreases slightly after hemifusion, while the max fluorescence intensity of PIP_2TMR increases following hemifusion.
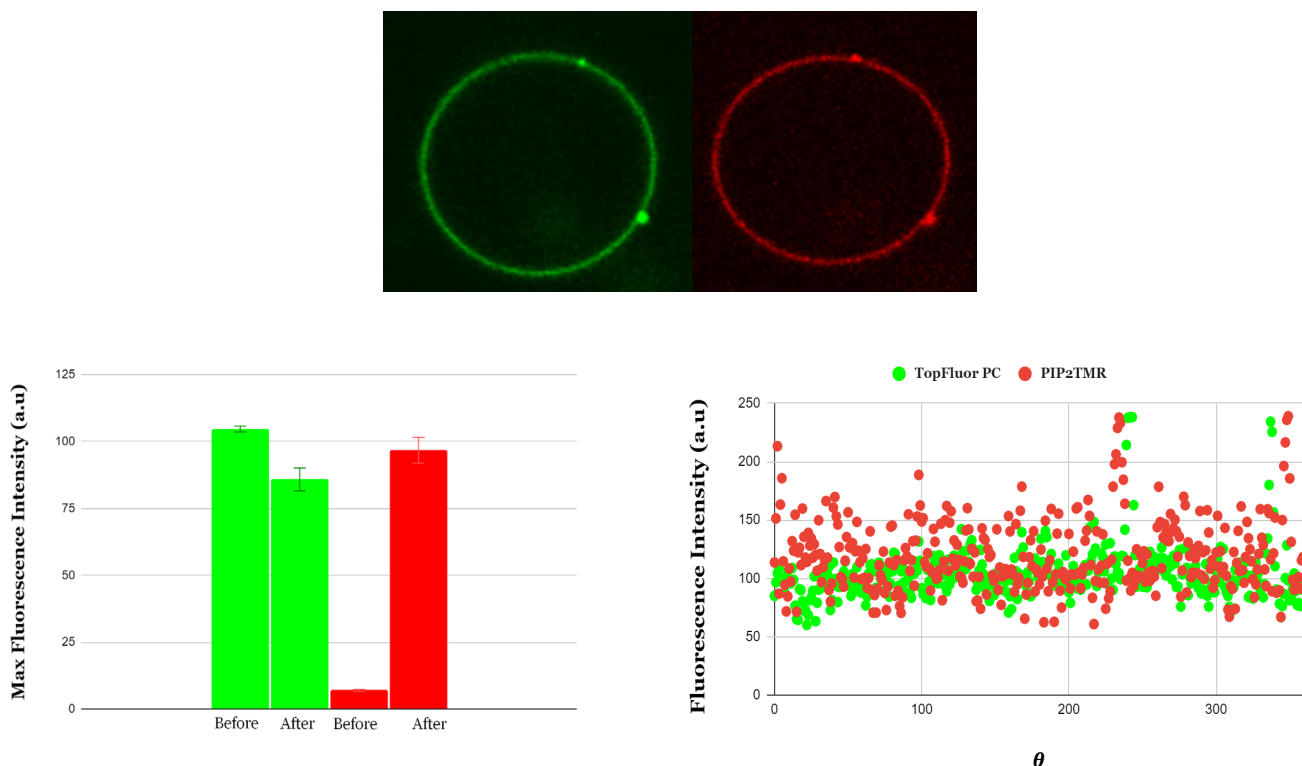

Figure 4. Quantification of Asymmetry of Non-Phase Separated GUVs. The inner leaflet was intended to contain the following concentrations: 40% DOPC, 40%DPPC, 20% cholesterol, and 0.05% TopFluor PC. Due to possible changes in the distribution of the lipid composition, there was no phase separation. Image of non-phase separated GUVs is shown at the top. **Right:** Fluorescence intensity profile of non-phase separated GUVs following hemifusion obtained by taking the intensity at points around the circumference of the GUV. **Left:** Max fluorescence intensity profile of the average intensity of a population of non-phase separated GUVs before and after hemifusion. Before n=6; after n=6. TopFluor PC shown in green; TopFluor TMR PI(4,5)P2 shown in red.

The quantification of fluorescence intensity in phase separated GUVs yielded a different result, and these results can be seen in Figure 5.
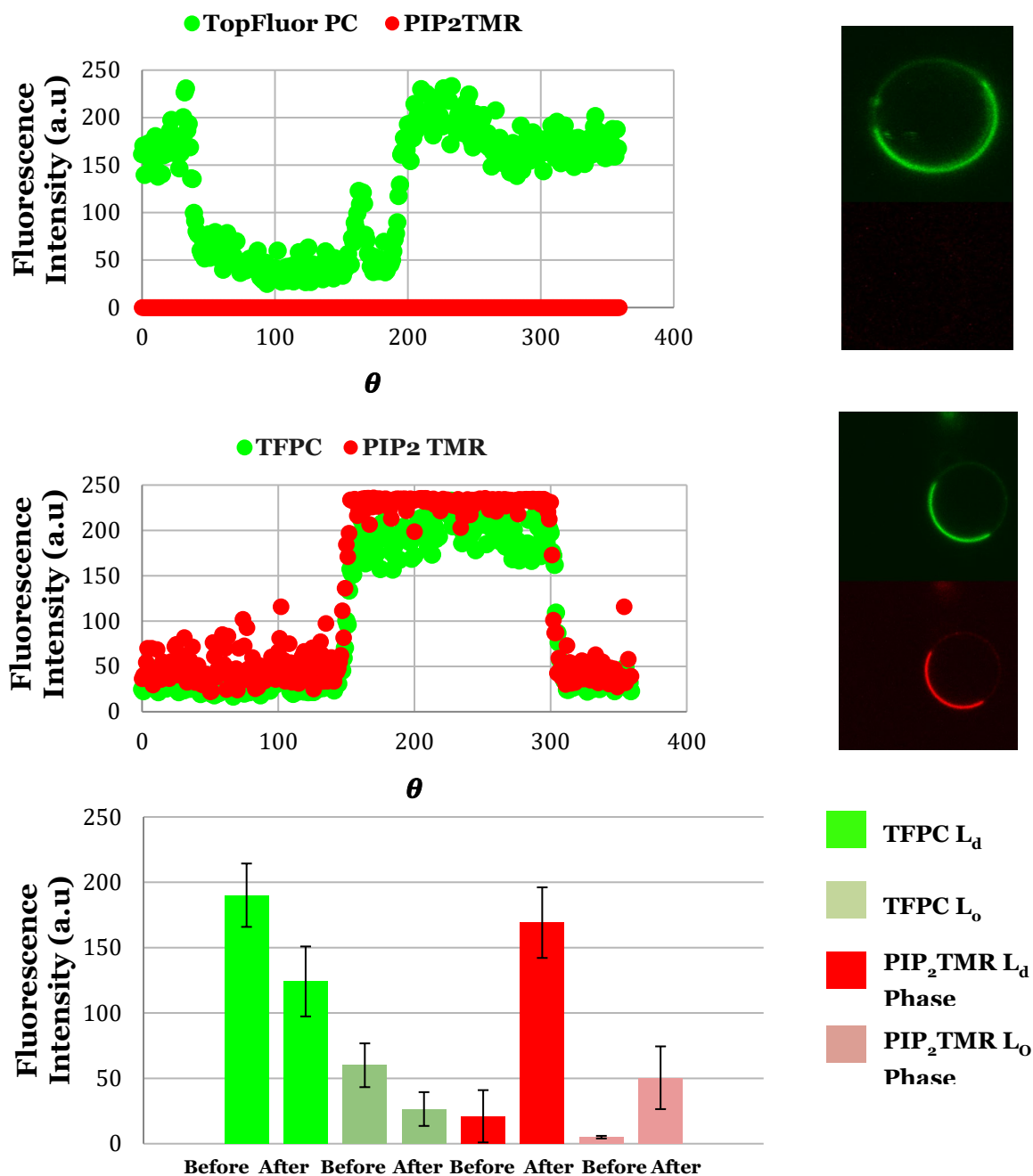
Figure 5. Quantification of Asymmetry of Phase Separated GUVs The inner leaflet was composed of 40% DOPC, 40%DPPC, 20% cholesterol, and 0.05% TopFluor PC. The outer leaflet was composed of 70% DOPC, 20% cholesterol, 5% PI(4,5)P$_2$ and 0.01% PI(4,5)P$_2$TMR. **Top:** The fluorescence intensity profile of a single phase separated GUV before hemifusion obtained by taking the intensity around the circumference of the GUV, image of GUV shown to the right. **Middle:** The fluorescence intensity profile of a single phase separated GUV following hemifusion. **Bottom:** The average fluorescence intensity profile of a population of phase separated GUVs before and after hemifusion. These profiles are separated into l$_o$ and l$_d$ phases for both TopFluor PC and PIP$_2$TMR.

The figure above, first shows an example of a phase separated GUV after hemifusion, which is indicated by the presence of the PIP$_2$TMR registering in the l$_d$ domain, like TopFluor PC. Additionally, the average maximum intensity of the GUV was taken in respect to both the TopFluor PC and PIP$_2$TMR and this can be observed in the middle chart. Lastly, the average intensities of the l$_o$ and l$_d$ domains was collected from a larger sample size of phase separated GUVs before (n=4) and after (n=24) hemifusion. When comparing the average intensity of the l$_d$ domain before and after hemifusion, the intensity decreased by approximately 35% and 56% in the l$_d$ and l$_o$ domain, respectively. While fluorescence intensity increases for PIP$_2$TMR in both domains.

4.4 Calcium Concentration

Calcium assays were used throughout the progress of this experiment to determine the concentration of calcium present during hemifusion and following the addition of EDTA to halt the process. The left image in Figure 6. depicts a standard curve created using the calcium sensitive dye Rhod-5N. This dye can detect calcium concentrations within the range of 0.1-10 mM. The λmax of Rhod-5N is 572 nm and thus the fluorescence intensity at 572 nm was recorded at various known calcium concentrations. The right image in Figure 6. depicts a graph plotting fluorescence intensity against calcium concentration, the fluorescence intensities existed in a range of 0-349 a.u. As shown in Figure 5., the sample of buffer collected before and after the addition of EDTA revealed that approximately 0.1 mM of Ca^{2+} was present in the solution before the addition of EDTA. Once the EDTA was added the Ca^{2+} concentration dropped to 0 mM as the EDTA chelated any remaining calcium.
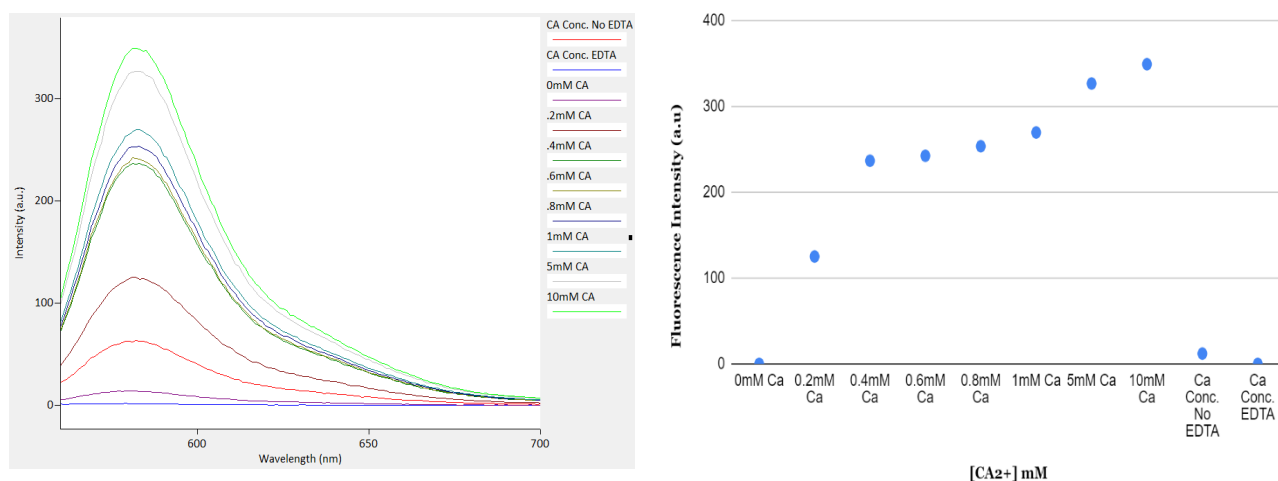

Figure 6. Calcium Concentration Determination. Left: Fluorescence emission traces of 0.04 μM Rhod-5N with concentrations of calcium ranging from 0-10 mM along with a sample of the aGUV buffer solution before and after EDTA is added. Rhod-5N exhibits a λmax of 572 nm. **Right:** Standard curve of calcium concentrations and a sample aGUV buffer solution before and after EDTA measured at 572 nm.

5. Discussion

5.1 Formation of Asymmetric GUVs

This project further demonstrated that phase separated GUVs can be fabricated using electroformation with a low salt buffer. In addition to phase separated GUVs, there was also the formation of non-phase separated GUV populations. The fabrication of non-phase separated GUVs is assumed to be caused by changes in the lipid raft mixture concentrations. Changes in concentration can be attributed to uneven spreading of the lipid mixture on the ITO slide or slight changes in concentration amounts due to measuring errors. The non-phase separated GUVs still serve as a method of measuring asymmetry following hemifusion.

Asymmetry in GUVs is indicated by a decrease in the fluorescence intensity of TopFluor PC after hemifusion occurs as the TopFluor PC now redistributes throughout the vesicle system following interleaflet coupling effects. A decrease in fluorescence intensity by 50% would indicate that there is 100% asymmetry within the GUVs. As shown in Figure 4., the fluorescence intensity of TopFluor PC only decreased by around 18% indicating that 100% asymmetry was not achieved

The sample size n=6, is relatively small and could account for the lack of observed asymmetry. Furthermore, the samples used in this portion were not from the same GUV population and the intensities could be affected by differences in lipid mixture distribution. In all of the produced aGUV populations hemifusion occurred rapidly and it is possible that some of the images captured had already begun the hemifusion process, which would account for inaccuracies in the change in fluorescence intensity before and after hemifusion. It is recommended that GUVs are added to the SLB with the calcium-containing buffer while the chamber is being imaged to capture GUV images before hemifusion can initiate. In isolated incidences, hemifusion would occur without the presence of calcium in the buffer solution, it is unclear how this occurred. There is potential that the buffers were introduced to minute amounts of calcium which then induced hemifusion.

A calcium assay was utilized to determine the concentration of calcium present after hemifusion was initiated and after EDTA was added to chelate the calcium and halt hemifusion. Following the performance of the calcium assay it was found that before the addition of EDTA there was approximately between 0.1-0.2 mM of Ca^{2+} present in the buffer solution. Following the addition of EDTA this concentration dropped to 0 mM.

The phase separated GUVs were analyzed differently from the non-phased separated GUVs. The fluorescence intensity of both the liquid-ordered and liquid-disordered phases were measured separately both before and after hemifusion. Deviating from the results collected from the non-phase separated GUVs, there was a more noticeable decrease in fluorescence intensity following hemifusion. The l_d phase experienced a 35% decrease in fluorescence intensity, while the l_o phase had a 56% decrease in intensity. These larger percent decreases indicate higher levels of asymmetry after hemifusion. The small sample size for the phase separated GUVs before hemifusion could potentially indicate inaccuracies in the collected data. A larger sample

size for GUVs before hemifusion would serve to further validate the data and fully indicate whether asymmetry was achieved.

5.2 Impacts of Cholesterol in Phosphoinositide-Containing Leaflet

The structure of cholesterol allows for it to promote the tight packing of sphingolipids/phospholipids [22-24]. The basis of the hypothesis for this thesis was built on the stabilizing nature of cholesterol, and it was believed that cholesterols ability to encourage the tight packing of other lipids would allow PIP_2 to register in the liquid-ordered region despite the electrostatic repulsion caused by its bulky acyl chains. Contrary to this belief, it was observed to be the opposite. The PIP_2 registered in the liquid-disordered region, which potentially indicates that the PIP_2 registration was dominated by the steric interactions between acyl chains rather than interactions with the sterol ring structure of cholesterol. An explanation for this observation could be related to the presence of the bulky fluorophore attached to the PIP_2, perhaps similar to the properties of TopFluor PC that promote partitioning into liquid-disordered domains, the fluorophore attached to PIP_2 dominates phase partitioning.

5.3 Future Directions

This thesis served as a method to further characterize asymmetric vesicle systems and following the results of this project it is important to conduct further experimentation to further characterize this system. Gaining more insight on the mechanisms of interleaflet coupling can aid in developing strategies to regulate pathways mediated by $PI(4,5)P_2$ and potentially allow for a method to induce PIP_2 clustering in specific regions of the plasma membrane to activate specific pathways. To advance this study, it is recommended to make the following adjustments to this project. First, due to the inducing of PIP_2 clustering by multivalent cations such as, Ca^{2+} or Mg^{2+}, a potential addition to this study would be to incorporate concentrations of Ca^{2+} into the lipid raft mixture or phosphoinositide-containing leaflet to encourage this clustering. Similar to the hypothesis of this thesis perhaps the presence of Ca^{2+} in the leaflets could stabilize the PIP_2 clustering events.

Secondly, an experiment should be run to determine if PIP_2 follows the same partitioning behavior of PIP_2TMR. Based on this project, it is unclear which domain the non-fluorescently labeled PIP_2 registers in compared to the fluorescently labeled PIP_2. Would this registration be dominated by headgroup interactions or acyl chain interactions? Lastly, conducting similar experiments after switching the inner and outer leaflet compositions would explore PIP_2 registration in more biologically accurate environments. As mentioned previously in this thesis, PIP_2 is located on the inner leaflet of the plasma membrane, therefore conducting a study with PIP_2 located on the inner leaflet of the model membrane system would be useful for further validating concepts regarding interactions between PIP_2 and other intracellular components.

6. Conclusion

In conclusion, this thesis further supported that asymmetric vesicles could be formed through hemifusion. This model membrane system can be utilized to further study the effects of interleaflet coupling. Furthermore, this project disproved my initial hypothesis. The presence of cholesterol in the phosphoinositide-containing leaflet did not encourage the registration of PIP_2 into the liquid-ordered domain. Potential experiments have been outlined to further characterize the mechanisms of interleaflet coupling and PIP_2 registration. These experiments have potential to increase our understanding of signaling pathways mediated by PIP_2 and provide insight on treating diseases connected to the upregulation/downregulation of these pathways.

Citations

1. Sunshine, H., & Iruela-Arispe, M. L. (2017). Membrane lipids and cell signaling. *Current Opinion in Lipidology, 28*(5), 408-413. doi:10.1097/mol.0000000000000443
2. Falkenburger, B. H., Jensen, J. B., Dickson, E. J., Suh, B., & Hille, B. (2010). Symposium Review: Phosphoinositides: Lipid regulators of membrane proteins. *The Journal of Physiology, 588*(17), 3179-3185. doi:10.1113/jphysiol.2010.192153
3. Witkowska, A., Jablonski, L. & Jahn, R. A convenient protocol for generating giant unilamellar vesicles containing SNARE proteins using electroformation. *Sci Rep* 8, 9422 (2018). https://doi.org/10.1038/s41598-018-27456-4
4. Simons, K., & Sampaio, J. L. (2011). Membrane organization and lipid rafts. *Cold Spring Harbor perspectives in biology*, *3*(10), a004697. https://doi.org/10.1101/cshperspect.a004697
5. Chan, Y. H., & Boxer, S. G. (2007). Model membrane systems and their applications. *Current opinion in chemical biology*, *11*(6), 581–587. https://doi.org/10.1016/j.cbpa.2007.09.020
6. Di Paolo, G., De Camilli, P. Phosphoinositides in cell regulation and membrane dynamics. *Nature* **443**, 651–657 (2006). https://doi.org/10.1038/nature05185
7. Kwik, J., Boyle, S., Fooksman, D., Margolis, L., Sheetz, M. P., & Edidin, M. (2003). Membrane cholesterol, lateral mobility, and the phosphatidylinositol 4,5-bisphosphate-dependent organization of cell actin. *Proceedings of the National Academy of Sciences of the United States of America*, *100*(24), 13964–13969. https://doi.org/10.1073/pnas.2336102100
8. Gamper, N., & Shapiro, M. S. (2007). Target-specific pip2signalling: How might it work? *The Journal of Physiology, 582*(3), 967-975. doi:10.1113/jphysiol.2007.132787
9. Owen, D. M., Magenau, A., Williamson, D., & Gaus, K. (2012). The lipid raft hypothesis revisited - new insights on raft composition and function from super-resolution fluorescence microscopy. *BioEssays, 34*(9), 739-747. doi:10.1002/bies.201200044
10. Grossmann, G., Opekarová, M., Malinsky, J., Weig-Meckl, I., & Tanner, W. (2007). Membrane potential governs lateral segregation of plasma membrane proteins and lipids in yeast. *The EMBO journal*, *26*(1), 1–8. https://doi.org/10.1038/sj.emboj.7601466
11. Lingwood, D., & Simons, K. (2009). Lipid rafts as a membrane-organizing principle. *Science, 327*(5961), 46-50. doi:10.1126/science.1174621
12. Dickson, E. J., & Hille, B. (2019). Understanding phosphoinositides: Rare, dynamic, and essential membrane phospholipids. *Biochemical Journal, 476*(1), 1-23. doi:10.1042/bcj20180022
13. Shukla, S., Jin, R., Robustelli, J., Zimmerman, Z. E., & Baumgart, T. (2019). PIP2 Reshapes Membranes through Asymmetric Desorption. *Biophysical journal*, *117*(5), 962–974. https://doi.org/10.1016/j.bpj.2019.07.047

14. Lupyan, D., Mezei, M., Logothetis, D. E., & Osman, R. (2010). A molecular dynamics investigation of lipid bilayer perturbation by PIP2. *Biophysical journal*, *98*(2), 240–247. https://doi.org/10.1016/j.bpj.2009.09.063

15. Pendaries, C., Tronchère, H., Plantavid, M., & Payrastre, B. (2003). Phosphoinositide signaling disorders in human diseases. *FEBS Letters, 546*(1), 25-31. doi:10.1016/s0014-5793(03)00437-x

16. Lombard J. (2014). Once upon a time the cell membranes: 175 years of cell boundary research. *Biology direct*, *9*, 32. https://doi.org/10.1186/s13062-014-0032-7

17. Nicolson, G. L. (2014). The Fluid—Mosaic model of Membrane Structure: Still relevant to understanding the STRUCTURE, function and dynamics of biological MEMBRANES after more than 40years. *Biochimica Et Biophysica Acta (BBA) - Biomembranes, 1838*(6), 1451-1466. doi:10.1016/j.bbamem.2013.10.019

18. Lin, Q., & London, E. (2014). Preparation of artificial plasma membrane mimicking vesicles with lipid asymmetry. *PLoS ONE, 9*(1). doi:10.1371/journal.pone.0087903

19. Wallace, E. J., Hooper, N. M., & Olmsted, P. D. (2006). Effect of hydrophobic mismatch on phase behavior of lipid membranes. *Biophysical Journal, 90*(11), 4104-4118. doi:10.1529/biophysj.105.062778

20. Kinnun, J. J., Bolmatov, D., Lavrentovich, M. O., & Katsaras, J. (2020). Lateral heterogeneity and domain formation in cellular membranes. *Chemistry and physics of lipids*, *232*, 104976. https://doi.org/10.1016/j.chemphyslip.2020.104976

21. Ackerman, D. G., & Feigenson, G. W. (2015). Lipid bilayers: clusters, domains and phases. *Essays in biochemistry*, *57*, 33–42. https://doi.org/10.1042/bse0570033

22. Korade, Z., & Kenworthy, A. K. (2008). Lipid rafts, cholesterol, and the brain. *Neuropharmacology, 55*(8), 1265-1273. doi:10.1016/j.neuropharm.2008.02.019

23. Stottrup, B. L., & Keller, S. L. (2006). Phase behavior of lipid monolayers containing DPPC and cholesterol analogs. *Biophysical journal*, *90*(9), 3176–3183. https://doi.org/10.1529/biophysj.105.072959

24. Lawrence, J. C., Saslowsky, D. E., Edwardson, J. M., & Henderson, R. M. (2003). Real-time analysis of the effects of cholesterol on lipid raft behavior using atomic force microscopy. *Biophysical journal*, *84*(3), 1827–1832. https://doi.org/10.1016/s0006-3495(03)74990-x

25. Slotte, J. (1995). Effect of sterol structure on molecular interactions and lateral domain formation in monolayers containing dipalmitoyl phosphatidylcholine. *Biochimica Et Biophysica Acta (BBA) - Biomembranes, 1237*(2), 127-134. doi:10.1016/0005-2736(95)00096-l

26. van Rheenen, J., Achame, E. M., Janssen, H., Calafat, J., & Jalink, K. (2005). PIP2 signaling in lipid domains: a critical re-evaluation. *The EMBO journal*, *24*(9), 1664–1673. https://doi.org/10.1038/sj.emboj.7600655

27. Johnson, C. M., & Rodgers, W. (2008). Spatial Segregation of Phosphatidylinositol 4,5-Bisphosphate (PIP(2)) Signaling in Immune Cell Functions. *Immunology, endocrine &*

metabolic agents in medicinal chemistry, *8*(4), 349–357.
https://doi.org/10.2174/187152208787169233

28. Nicolau, D. V., Jr, Burrage, K., Parton, R. G., & Hancock, J. F. (2006). Identifying optimal lipid raft characteristics required to promote nanoscale protein-protein interactions on the plasma membrane. *Molecular and cellular biology*, *26*(1), 313–323. https://doi.org/10.1128/MCB.26.1.313-323.2006

29. Enoki TA, Feigenson GW. Asymmetric Bilayers by Hemifusion: Method and Leaflet Behaviors. Biophys J. 2019 Sep 17;117(6):1037-1050. doi: 10.1016/j.bpj.2019.07.054. Epub 2019 Aug 21. PMID: 31493862; PMCID: PMC6818168.

30. Hunker, Olivia. Fabrication and Characterization of Asymmetric Phosphoinositide-containing Vesicles

31. Attwood, S. J., Choi, Y., & Leonenko, Z. (2013). Preparation of DOPC and DPPC Supported Planar Lipid Bilayers for Atomic Force Microscopy and Atomic Force Spectroscopy. *International journal of molecular sciences*, *14*(2), 3514–3539. https://doi.org/10.3390/ijms14023514

32. Hardy, G. J., Nayak, R., & Zauscher, S. (2013). Model cell membranes: Techniques to form complex biomimetic supported lipid bilayers via vesicle fusion. *Current Opinion in Colloid & Interface Science, 18*(5), 448-458. doi:10.1016/j.cocis.2013.06.004

33. Åkesson, A., Lind, T., Ehrlich, N., Stamou, D., Wacklin, H., & Cárdenas, M. (2012). Composition and structure of mixed phospholipid supported bilayers formed By POPC And dppc. *Soft Matter, 8*(20), 5658. doi:10.1039/c2sm00013j

34. Fujimoto, T., & Parmryd, I. (2017). Interleaflet coupling, pinning, and Leaflet ASYMMETRY—MAJOR players in plasma MEMBRANE Nanodomain Formation. *Frontiers in Cell and Developmental Biology, 4*. doi:10.3389/fcell.2016.00155

35. Conway, S. J., Gardiner, J., Grove, S. J., Johns, M. K., Lim, Z., Painter, G. F., . . . Holmes, A. B. (2010). Synthesis and biological evaluation of phosphatidylinositol phosphate affinity probes. *Org. Biomol. Chem., 8*(1), 66-76. doi:10.1039/b913399b

36. Shi, X., Kohram, M., Zhuang, X., & Smith, A. W. (2016). Interactions and Translational dynamics of PHOSPHATIDYLINOSITOL Bisphosphate (PIP2) lipids in Asymmetric lipid bilayers. *Langmuir, 32*(7), 1732-1741. doi:10.1021/acs.langmuir.5b02814.s001

37. Braunger, J. A., Kramer, C., Morick, D., & Steinem, C. (2013). Solid supported Membranes doped With PIP2: Influence of ionic strength and pH on BILAYER formation and MEMBRANE ORGANIZATION. *Langmuir, 29*(46), 14204-14213. doi:10.1021/la402646k

38. McLaughlin, S., Wang, J., Gambhir, A., & Murray, D. (2002). PIP2and Proteins: Interactions, Organization, and Information Flow. *Annual Review of Biophysics and Biomolecular Structure*, *31*(1), 151–175. https://doi.org/10.1146/annurev.biophys.31.082901.134259

39. Wen, Y., Vogt, V. M., & Feigenson, G. W. (2018). Multivalent Cation-Bridged PI(4,5)P2 Clusters Form at Very Low Concentrations. *Biophysical Journal*, *114*(11), 2630–2639. https://doi.org/10.1016/j.bpj.2018.04.048

40. Levental, I., Christian, D. A., Wang, Y. H., Madara, J. J., Discher, D. E., & Janmey, P. A. (2009). Calcium-dependent lateral organization in phosphatidylinositol 4,5-bisphosphate (PIP2)- and cholesterol-containing monolayers. *Biochemistry*, *48*(34), 8241–8248. https://doi.org/10.1021/bi9007879